

IMPORTANCE OF CLUSTER STRUCTURAL EVOLUTION IN USING X-RAY AND SZE
GALAXY CLUSTER SURVEYS TO STUDY DARK ENERGYSUBHABRATA MAJUMDAR¹ & JOSEPH J MOHR^{1,2}submitted to *ApJ* June 14, 2002

ABSTRACT

We examine the prospect of measuring the dark energy equation of state parameter ‘ w ’ within the context of the still uncertain redshift evolution of galaxy cluster structure. We show that for both an X-ray and an SZE survey the constraints on w degrade by roughly a factor of 3 when one accounts for the possibility of non-standard cluster evolution. With follow-up mass measurements it is possible to measure cluster evolution, improving constraints on cosmological parameters. We examine scenarios where 1%, 10% and 100% of detected clusters are followed up with mass measurements, showing that even a modest follow-up program can enhance the final cosmological constraints. In the best case scenario of full follow-up with an uncertainty of 30% on individual cluster mass measurements, one proposed large solid angle SZE cluster survey can deliver a 1σ error of $\sim 8\%$ on ‘ w ’.

Subject headings: cosmic microwave background — galaxies: clusters — cosmology: theory

1. INTRODUCTION

Galaxy clusters have been used extensively to determine the cosmological matter density parameter and the amplitude of density fluctuations. More recently, it has been recognized that with current instrumentation it is possible to use surveys of galaxy clusters extending to redshifts $z > 1$ to precisely study the amount and nature of the dark energy (Haiman et al. 2001; Holder et al. 2001; Weller et al. 2001).

Clusters are promising tools for precision cosmological measurements, because they exist during the epoch of dark energy domination, and their use is complementary to studies of cosmic microwave background (CMB) anisotropy and SNe Ia distance measurements (Haiman et al. 2001; Levine et al. 2002; Hu & Kravstov 2002). In this paper we examine the effects of cluster structural evolution on cosmological constraints from cluster surveys, finding that current survey projections that ignore this evolution uncertainty overstate the cosmological sensitivity of the survey. Furthermore, we examine the effects of survey follow-up to measure masses, demonstrating that an appropriately designed survey can overcome this evolution uncertainty.

In §2 we describe two representative surveys and survey follow-up. Section 3.1 contains a description of our estimates of the survey sensitivity when follow-up is included as well as a description of our fiducial model. Results are presented in §4 and discussed further in §5.

2. FUTURE GALAXY CLUSTER SURVEYS

We begin our study of using cluster surveys to probe dark energy by computing the redshift distribution of detectable clusters,

$$\frac{dN}{dz} = \Delta\Omega \frac{dV}{dzd\Omega}(z) \int_0^\infty f(M) \frac{dn(z)}{dM} dM \quad (1)$$

where $dV/dzd\Omega$ is the comoving volume element, $(dn/dM)dM$ is the comoving density of clusters of mass

M , and $f(M)$ is the cluster selection function for the survey. In this analysis we take $f(M)$ to be a step function at some limiting mass M_{lim} , which corresponds to the mass of a cluster that lies at the survey detection threshold. We use the cluster mass function dn/dM determined from structure formation simulations (Jenkins et al. 2001).

In practice surveys select clusters using observables like the X-ray flux, SZE flux, galaxy light or weak lensing shear. Thus, in addition to the ingredients above, one requires a virial mass–observable relation (like $M-L_x$, $M-L_{sz}$ or $M-\gamma_t$). A central feature of these mass–observable relations is that they evolve with redshift due to the increasing density of the universe at earlier times (and the changing ratio of distance to lens and source in the case of weak lensing). Within standard structure formation models, galaxy clusters form self-similarly, and so there are standard evolution models for each mass–observable relation (e.g. Bryan & Norman 1998; Mohr et al. 2000; Evrard et al. 2002). However, given the central importance of cluster mass estimates in using surveys to study dark energy, we can only regard these standard structure formation models as a guide; ultimately, one needs to determine the evolution of cluster structure observationally. In this paper we examine the effects that non-standard redshift evolution of cluster structure would have on our ability to use cluster surveys to study the dark energy.

2.1. An X-ray and an SZE Survey

We examine two high yield surveys: (i) a 10^4 deg² flux limited X-ray survey proposed as part of the DUET mission to the NASA Medium-class Explorer Program, and (ii) a 4,000 deg² SZE survey to be carried out with a proposed ~ 8 m South Pole Telescope (SPT). Figure 1 contains a plot of the redshift distribution and limiting mass for both surveys.

We model the DUET X-ray survey as having a bolometric flux limit of $f_x > 1.25 \times 10^{-13}$ erg/s/cm² (corresponding to $f_x > 5 \times 10^{-14}$ erg/s/cm² in the 0.5:2 keV

¹Department of Astronomy, University Of Illinois, 1002 West Green St., Urbana, IL 61801²Department of Physics, University Of Illinois, 1002 West Green St., Urbana, IL 61801

band). For our fiducial cosmological model (see §3.2 below) this survey yields $\sim 16,000$ detected clusters, consistent with the known X-ray log N –log S relation for clusters (e.g. Gioia et al. 2001). For our mass–observable relation, we adopt a bolometric X-ray luminosity–mass relation

$$f_x(z)4\pi d_L^2 = A_x M_{200}^{\beta_x} E^2(z) (1+z)^{\gamma_x} \quad (2)$$

where f_x is the observed flux in units of $\text{erg s}^{-1}\text{cm}^{-2}$, d_L is in units of Mpc, M_{200} is in units of $10^{15} M_\odot$ and $H(z) = H_0 E(z)$. We convert M_{200} to $M(z)$, the halo mass appropriate for our mass function at redshift z using a halo model (Navarro et al. 1997). Our standard evolution model ignores the $T^{1/2}$ dependence of the bolometric bremsstrahlung radiation, because X-ray surveys detect clusters using detected photons rather than detected energy. We introduce the possibility of non-standard evolution of the mass–observable relation with the parameter γ_x . We take $\gamma_x = -0.2$ to be consistent with the lack of evolution in the luminosity–temperature relation to intermediate redshift (e.g. Mushotzky & Scharf 1997), and we choose $\beta_x = 1.807$ and $\log A_x = -3.926$, consistent with observations (Reiprich & Böhringer 2002). The overall h scaling of the limiting mass is $h^{-1.11}$.

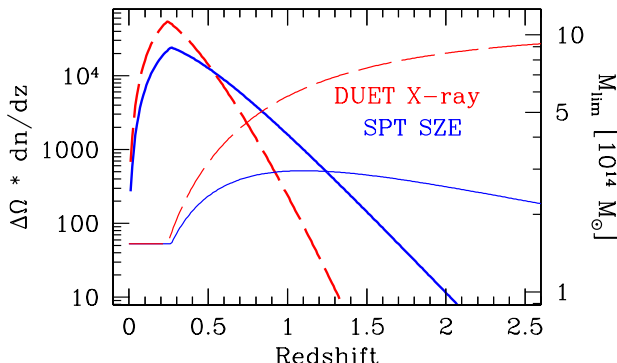


FIG. 1.— The cluster redshift distribution (heavy line) and mass limit (light line) of the 10^4 deg^2 DUET X-ray survey (dashed) and the $4,000 \text{ deg}^2$ South Pole Telescope (SPT) SZE survey (solid). The surveys are flux limited ($f_x > 1.25 \times 10^{-13} \text{ erg/s/cm}^2$ and $f_{sz} > 5 \text{ mJy at 150 GHz}$), and we impose a minimum cluster mass of $1.54 \times 10^{14} M_\odot$.

We model the SPT SZE survey as a flux limited survey with $f_{sz} > 5 \text{ mJy at 150 GHz}$. Within our fiducial cosmological model this survey would yield $\sim 10,000$ clusters with measured fluxes. The mass–observable relation is

$$f_{sz}(z)d_A^2 = 3.781 f(\nu) f_{ICM} T M_{200} (1+z)^{\gamma_{sz}} \\ M_{200} = A_{sz} \frac{(k_B T)^{\beta_{sz}}}{E(z)} \quad (3)$$

where $f(\nu)$ is the frequency dependence of the SZE distortion, f_{sz} is the observed flux in mJy, T is in Kelvin, M_{200} is in units of $10^{15} M_\odot$, $f_{ICM} = 0.12$ (e.g Mohr et al. 1999) and d_A is in units of Mpc (see Diego et al. 2002). We use $\log A_{sz} = 13.466$, $\beta_{sz} = 1.48$ (Finoguenov et al. 2001) and $\gamma_{sz} = 0$ to model standard structure evolution. In this form, the overall h scaling of the limiting mass is $h^{-1.61}$.

A generic problem with flux limited surveys is that at low redshift the implied mass limit drops well below those masses corresponding to galaxy clusters. The flux from a nearby object is spread over a much larger portion of the sky, and surface brightness selection effects become important. We model these complications by imposing a

minimum cluster mass of $10^{14} h^{-1} M_\odot$. This lower limit on the survey mass limit is readily apparent below $z \sim 0.25$ in Fig 1.

2.2. Follow-up of Large Solid Angle Surveys

The redshift distribution of clusters contains far more cosmological information than the surface density of clusters (Haiman et al. 2001) or the angular correlation function (e.g. Komatsu & Seljak 2002). Thus, in both these surveys each detected cluster will be followed up with multi-band optical and near-IR photometry to provide photometric redshift estimates. These same data can be used to estimate cluster masses through their weak lensing effects on background galaxies (Bartelmann 2001) and the total detected light from cluster galaxies.

In addition, some of these clusters can be followed up with detailed X-ray, SZE or galaxy spectroscopic observations that allow one to measure the mass-like quantity $M_f(\theta) = M(\theta)/d_A$, which we will refer to as the follow-up mass. As an example, in the case of follow-up X-ray observations that deliver the projected ICM temperature profile and surface brightness profile, it is straightforward to extract the underlying ICM density $\rho(d_A \theta)$ and temperature profile $T(d_A \theta)$ to then estimate the follow-up mass M_f as

$$M_f(\theta) = -\theta \frac{k_B T(\theta)}{G \mu m_p} \left(\frac{d \ln \rho}{d \ln \theta} + \frac{d \ln T}{d \ln \theta} \right) \quad (4)$$

where m_p is the proton mass, k_B is Boltzmann constant, G is Newton constant, and the ICM number density $n \equiv \rho/\mu m_p$. Note that only the *shape* of the ICM density profile is required. At fixed redshift, this follow-up would produce an M_f – f_x of M_f – f_{sz} relation which would provide direct constraints on the structural evolution of the clusters. The parameter sensitivity of these scaling relation observations can exhibit quite different degeneracies than for the cluster redshift distribution, making the two observables complementary. In §3.1 below, we describe how these survey follow-up observations are included in our estimates of the cosmological sensitivity of the survey.

3. COSMOLOGICAL SENSITIVITY OF A SURVEY

3.1. Fisher Matrix Technique

We employ the Fisher matrix technique to probe the relative sensitivities of two cluster surveys to different cosmological and cluster structural parameters. The Fisher matrix information for a data set (see Tegmark et al. 1997; Eisenstein et al. 1998) is defined as $F_{ij} \equiv \langle \frac{\partial^2 \ln \mathcal{L}}{\partial p_i \partial p_j} \rangle$, where \mathcal{L} is the likelihood for an observable ($\frac{dN}{dz}$ for the survey and M_f for the followup) and p_i describes our parameter set. The inverse F_{ij}^{-1} describes the best attainable covariance matrix [C_{ij}] for error measurement on these parameters. The diagonal terms in [C_{ij}] then gives the error on each of our parameters. In calculating the errors, we have added the Fisher matrix for the followup (F_{ij}^f), the Fisher matrix for the survey (F_{ij}^s) and the external priors mentioned above.

We construct the F_{ij}^s following Holder et al. (2001) as

$$F_{ij}^s = \Sigma_n \frac{\partial dN/dz}{\partial p_i} \frac{\partial dN/dz}{\partial p_j} \frac{1}{dN/dz}, \quad (5)$$

TABLE 1
ESTIMATED PARAMETER CONSTRAINTS

Description	Ω_M	Ω_{tot}	σ_8	w	h	n	Ω_B	$\log A$	β	γ
<i>Priors</i>		0.0100			0.0500	0.0500	fixed			
<i>SPT SZE Survey</i>										
Std Evolution	0.0126	0.0068	0.0132	0.1289	0.0496	0.0489	-			
Non-Std Evolution	0.0227	0.0099	0.0262	0.3184	0.0499	0.0497	-	0.3802	0.0178	0.7375
+ 1% Followup	0.0201	0.0085	0.0156	0.1789	0.0497	0.0489	-	0.3331	0.0160	0.1933
+ 10% Followup	0.0144	0.0074	0.0102	0.1263	0.0496	0.0488	-	0.2103	0.0102	0.1016
+ 100% Followup	0.0097	0.0064	0.0057	0.0828	0.0496	0.0488	-	0.0821	0.0039	0.0526
<i>DUET X-ray Survey</i>										
Std Evolution	0.0123	0.0082	0.0102	0.1141	0.0495	0.0488	-			
Non-Std Evolution	0.0215	0.0098	0.0298	0.3173	0.0496	0.0490	-	0.1825	0.0119	0.9633
+ 1% Followup	0.0188	0.0094	0.0204	0.2349	0.0496	0.0489	-	0.1771	0.0119	0.5808
+ 10% Followup	0.0167	0.0091	0.0134	0.1777	0.0495	0.0487	-	0.1715	0.0118	0.2602
+ 100% Followup	0.0127	0.0087	0.0089	0.1301	0.0494	0.0484	-	0.1585	0.0113	0.1450

where we sum over n redshift bins of size $\Delta z = 0.01$ to $z_{max} = 3.0$. The Fisher matrix for the followup is constructed as

$$F_{ij}^f = \Sigma_n \frac{\partial M_f}{\partial p_i} \frac{\partial M_f}{\partial p_j} \frac{N_n}{\sigma_{M_f}^2} \quad (6)$$

where N_n is the number of clusters used for follow-up in bin n and $\sigma_{M_f} = 0.3M_f$ is our characteristic uncertainty in follow-up mass measurements. In calculating (F_{ij}^f) we assume follow-up clusters are chosen from the survey sample randomly with respect to redshift (e.g. $N_n = f dN/dz$, where f is the fraction of detected clusters followed up), and we ignore the flux distribution at a particular redshift.

3.2. Fiducial Cosmology and External Constraints

The fiducial cosmological parameters of our model are $h = 0.65$, $\Omega_M = 0.3$, $\Omega_{tot} = \Omega_M + \Omega_E = 1$, $w = -1$, $n = 0.96$, $\Omega_B = 0.047$, and a COBE normalized $\sigma_8 = 0.72$ (Bunn & White 1997; Burles & Tytler 1998; Grego et al. 2001; Mohr et al. 1999; Netterfield et al. 2001; Pryke et al. 2001). Note that we use a rather low value of σ_8 , which is consistent with the recent 2dF analysis (Lahav et al. 2002). Because the expected number density of clusters is very sensitive to the value of σ_8 , our fiducial SZE survey has fewer clusters when compared to previous studies (Holder et al. 2001).

Cosmological constraints from cluster surveys are complementary to constraints from SNe Ia distance measurements and observations of the anisotropy of cosmic microwave background. This is particularly true when it comes to using cluster surveys to measure the dark energy equation of state parameter w (Haiman et al. 2001). In combination with precise CMB constraints on the curvature ($\Omega_k = 0$), cluster surveys enable precise measurements of the dark energy equation of state; however, when curvature is allowed to depart from zero— even slightly—the cluster constraints on w weaken considerably. For a prior of $\sigma_k = 0.001$, the constraints assuming standard evolution on w (Ω_M) are 0.0581 (0.0119), whereas for $\sigma_k = 0.01$ the constraints are 0.1289 (0.0126).

For the analysis presented here, we adopt relatively conservative priors from future CMB anisotropy studies and distance measurements. We assume the power spectrum index n will be known to $\sigma_n = 0.05$, the Hubble parameter will be known to $\sigma_h = 0.05$, and the total density parameter Ω_{tot} will be known to $\sigma_k = 0.01$. In addition, we take the baryon density parameter to be fixed

at $\Omega_B = 0.047$. For reasonable values of Ω_B , surveys are affected only through minor effects on the transfer function for density perturbations (Eisenstein & Hu 1998; Levine et al. 2002). Finally, we neglect the possibility of a variation in the equation of state parameter w (Weller et al. 2001).

4. COSMOLOGICAL PARAMETER CONSTRAINTS

4.1. Importance of Non-Standard Evolution

Figure 2 contains joint constraints on Ω_m and w for the two surveys. For each survey we show constraints with and without non-standard evolution in the cluster scaling relations. Focus first on the constraints from dN/dz alone with standard evolution (solid line) and non-standard evolution (dotted line). Clearly, allowing for the possibility of non-standard evolution dramatically weakens our constraints on w . Calculations that ignore the possibility of non-standard evolution lead to over-optimistic estimates of potential cosmological constraints. The degradation in our w constraints is due to increased freedom in the mass-observable relations afforded by the evolution parameters γ_x and γ_{sz} .

Table 1 contains a listing of errors on all cosmological and mass-observable relation parameters. In the standard evolution case, the SZE and X-ray surveys compare favorably, yielding 1σ absolute errors on w (Ω_M) of 0.129 and 0.114 (0.0126 and 0.0123), respectively. However, when one takes into account the possibility of non-standard evolution, the constraints on w weaken by almost a factor of 3 to ~ 0.32 in both surveys; Ω_M constraints weaken by close to a factor of 2 to 0.022. The constraints from dN/dz on $\gamma_{sz/x}$ are very weak at 0.73 and 0.96, respectively; this large uncertainty in the evolution of the mass-observable relation leads to the weakened sensitivity of dN/dz to cosmological parameters.

The importance of evolution in interpreting the cluster redshift distribution contrasts somewhat with the results of the Levine et al. (2002) study, which showed that prior knowledge of the normalization of the mass-observable relation has only a weak effect on the cosmological sensitivity of cluster surveys (see also Diego et al. 2001). In their study, they only considered the standard evolution model. Within the context of uncertain evolution of the mass-observable relation one needs observations in addition to dN/dz to determine the evolution parameter γ and regain

sensitivity to the equation of state parameter w . Next we examine the effects of including follow-up mass measurements.

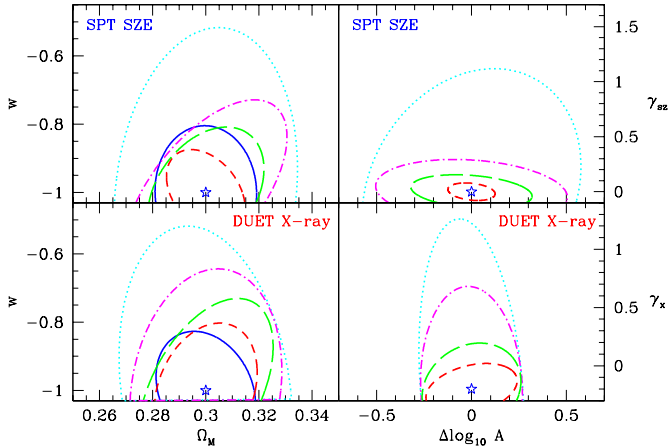


FIG. 2.— Constraints on w and Ω_M (left) and the mass-observable relation normalization A and redshift evolution $(1+z)^\gamma$ (right) for an SZE (above) and an X-ray survey (below). The star marks the fiducial model. Contours denote joint 1σ constraints in five scenarios: constraints from dN/dz where (i—solid) cluster evolution is known (left column only) and (ii—dotted) evolution is unknown, constraints from dN/dz and follow-up mass measurements for (iii—dot-dashed) 1% of sample, (iv—long dashed) 10% of sample, and (v—short dashed) 100% of sample. The follow-up mass measurements are estimated to have fractional uncertainties of 30%.

4.2. Effects of Follow-up Mass Measurements

We examine the effects of follow-up masses by examining 1%, 10% and 100% follow-up in both surveys. Figure 2 contains joint confidence contours for these three cases (1%—dot-dashed, 10%—long dashed, 100%—short dashed). It is clear from this figure that even very limited follow-up of 1% of the detected clusters can significantly impact the parameter uncertainties. Follow-up of the full sample allows one to regain or even improve upon the constraints possible from dN/dz alone when one assumes that evolution of the mass-observable relation is perfectly known. Note that follow-up has a more significant effect on the SZE survey constraints. This can be traced to our assumption that the redshift distribution of follow-up mass measurements matches the redshift distribution of the full survey. The higher redshift follow-up measurements contain more information about evolution, and the SZE survey probes to higher redshift than does the X-ray survey (see Fig. 1). Survey strategists should consider a follow-up program that targets predominantly high redshift clusters, but having evolution information over the entire redshift range of the survey is critical to testing the form of the evolution model.

Table 1 contains a listing of the effects of follow-up on all parameters. It is clear that follow-up mass measurements dramatically reduce the projected uncertainties on cosmological and scaling relation parameters. As is evident from the last column in the table, even a modest followup of 10% of the clusters reduces the uncertainty on γ from 0.96 to 0.58 for the X-Ray case and 0.79 to 0.19 for the SZE survey. With full follow-up, the constraint on w shrinks from 0.31 to 0.08 in the SZE and 0.13 in the X-ray survey. Even with follow-up of only 100 clusters in the SZE survey, one reduces the error on w by half.

In Fig. 2 (right column) we show the constraints on the

mass-observable relation normalization A and the evolution parameter γ for the four cases: no followup (dotted) and a followup of 1% (dot-dashed), 10% (long dashed) and 100% (short dashed) of the clusters. Follow-up has strikingly different effects in the SZE and X-ray surveys. Follow-up in the SZE survey is much more effective at constraining the evolution parameter γ_{sz} , due to the deeper redshift of this survey. The differences in the constraints on $\log_{10} A$ generally reflect the different definitions of the normalization and its relationship to halo mass (see Eqns 2 & 3). We emphasize again that in the partial follow-up case one should preferentially follow-up those clusters that will have the largest impact on parameter constraints.

5. DISCUSSION AND CONCLUSIONS

Any attempt to measure the dark energy equation of state w with cluster surveys will require (i) a strong external prior on the curvature (presumably from CMB anisotropy studies) and (ii) an understanding of the evolution of the relation between cluster halo mass and observable properties like the X-ray luminosity, SZE luminosity, galaxy light or weak lensing shear. We have examined the effects of current uncertainties about cluster structural evolution; for two recently proposed cluster surveys the estimated constraints on w are ~ 3 times weaker than if one assumes full knowledge of cluster evolution. Constraints on other interesting cosmological parameters are also weakened (see Table 1).

Follow-up observations to measure cluster masses directly will enable one to solve for cluster structure evolution and to enhance cosmological constraints. We have examined the effects of follow-up mass observations from hydrostatic or dynamical methods, and we find that even modest follow-up of 1% of the cluster sample can improve survey constraints. Full follow-up with mass measurements that are 30% uncertain, on average, provide cosmological constraints that match or surpass those possible through dN/dz alone with full knowledge of cluster evolution. Full follow-up with weak lensing mass measurements is currently being planned for the SPT SZE survey.

One interesting feature of our analysis is the orientation of the elliptical constraints on w and Ω_M (see Fig. 2). In general, the rotation of the parameter degeneracy can be understood as the result of competing effects of changes in the volume element and the growth factor as parameters vary. Variations in w (and Ω_M) affect the survey yield in different ways at different redshifts, and so the w — Ω_M degeneracy depends on the redshift distribution of a particular survey. Rotations of parameter degeneracies occur as the maximum redshift of the survey is varied (Levine et al. 2002; Hu & Kravstov 2002). We have further found that changing the prior on Ω_{tot} and changing the degree of mass follow-up on a survey also result in rotations of the parameter degeneracy. This behavior has interesting implications for the design of cluster surveys that are optimally complementary to CMB anisotropy and SNe Ia distance measurements, and it deserves further study.

SM thanks Ben Wandelt and Shiv Sethi for helpful conversations. JM thanks Zoltan Haiman for many fun discussions on cluster surveys. This work has been supported by NASA Long Term Space Astrophysics grant

NAG5-11415 and *Chandra* X-ray Observatory archival grant AR1-2002X, awarded through the Smithsonian As-

trophysical Observatory.

REFERENCES

Bartelmann, M. 2001, A&A, 370, 754
 Bryan, G. L. & Norman, M. L. 1998, ApJ, 495, 80
 Bunn, E. F. & White, M. 1997, ApJ, 480, 6
 Burles, S. & Tytler, D. 1998, ApJ, 507, 732
 Diego, J. M., Martínez-González, E., Sanz, J. L., Benítez, N., & Silk, J. 2002, MNRAS, 331, 556
 Diego, J. M., Martínez-González, E., Sanz, J. L., Cayón, L., & Silk, J. 2001, MNRAS, 325, 1533
 Eisenstein, D. J. & Hu, W. 1998, ApJ, 496, 605
 Eisenstein, D. J., Hu, W., & Tegmark, M. 1998, ApJ, 504, L57
 Evrard et al. 2002, ApJ, in press (astro-ph/0110246)
 Finoguenov, A., Reiprich, T. H., & Böhringer, H. 2001, A&A, 368, 749
 Gioia, I. M., Henry, J. P., Mullis, C. R., Voges, W., Briel, U. G., Böhringer, H., & Huchra, J. P. 2001, ApJ, 553, L105
 Grego, L., Carlstrom, J. E., Reese, E. D., Holder, G. P., Holzapfel, W. L., Joy, M. K., Mohr, J. J., & Patel, S. 2001, ApJ, 552, 2
 Haiman, Z., Mohr, J. J., & Holder, G. P. 2001, ApJ, 553, 545
 Holder, G., Haiman, Z., & Mohr, J. J. 2001, ApJ, 560, L111
 Hu, W. & Kravstov, A. 2002, ApJ, submitted astro-ph/0203169
 Jenkins, A., Frenk, C. S., White, S. D. M., Colberg, J. M., Cole, S., Evrard, A. E., Couchman, H. M. P., & Yoshida, N. 2001, MNRAS, 321, 372
 Komatsu, E. & Seljak, U. 2002, MNRAS, submitted (astro-ph/0205468)
 Lahav et al. 2002, MNRAS, in press (astro-ph/0112162)
 Levine, E. S., Schulz, A. E., & White, M. 2002, ApJ, submitted (astro-ph/0204273)
 Mohr, J. J., Mathiesen, B., & Evrard, A. E. 1999, ApJ, 517, 627
 Mohr, J. J., Reese, E. D., Ellingson, E., Lewis, A. D., & Evrard, A. E. 2000, ApJ, 544, 109
 Mushotzky, R. F. & Scharf, C. A. 1997, ApJ, 482, L13
 Navarro, J. F., Frenk, C. S., & White, S. D. M. 1997, ApJ, 490, 493
 Netterfield et al. 2001, ApJ, submitted (astro-ph/0104460)
 Pryke, C., Halverson, N. W., Leitch, E. M., Kovac, J., Carlstrom, J. E., Holzapfel, W. L., & Dragovan, M. 2001, ApJ, submitted (astro-ph/0104490)
 Reiprich, T. H. & Böhringer, H. 2002, ApJ, 567, 716
 Tegmark, M., Taylor, A. N., & Heavens, A. F. 1997, ApJ, 480, 22+
 Weller, J., Battye, R., & Kniessl, R. 2001, astro-ph (0110353)